SAND2024-09862C

Impact of Collector Network Aggregation of Solar and Type 4 Wind Farms for Short Circuit Studies

Samuel T. Ojetola, Trupal R. Patel, Matthew J. Reno
Electric Power System Research
Sandia National Laboratories
Albuquerque, NM, USA
sojetol@sandia.gov, tpatel@sandia.gov, mjreno@sandia.gov

Shah Mohazzem Hossain, Sukumar Brahma
Holcombe Department of ECE
Clemson University
Clemson, SC, USA
shossai@clemson.edu, sbrahma@clemson.edu

2024 IEEE Green Technologies Conference (GreenTech) | 979-8-3503-0858-7/24/$31.00 ©2024 IEEE | DOI: 10.1109/GREENTECH58819.2024.10520373

***Abstract*—With increasing interest in renewable energy generation, grid integration of Distributed Energy Resources (DERs), such as solar photovoltaic (PV) plants, wind turbine farms, and energy storage systems have become more common. These connected DERs usually consist of inverters, pad-mounted transformers, and collector feeders. As the size and number of PV plants and wind farm increases, it becomes challenging for power system planners to study their impact on the power system, since it is not practical to represent all individual inverters, transformers and feeders to conduct simulations. This paper examines the impact of aggregating the collector network in a solar farm and a type-4 wind farm, employing two aggregation techniques. The first represents the collector network with an equivalent impedance and a shunt capacitance, while the second assumes that the impact of the collector is negligible.**

***Index Terms*—aggregation, collector feeder, distribution network, equivalence, inverter, solar farm, wind farm.**

I. Introduction

WIND and solar energy are two of the three fastest growing renewable energy sources in the United States [1], [2]. In 2020 and 2021, over 16 GW and 13 GW of wind capacity was installed in the US respectively. Solar capacity has grown at an average of 24% annually over the last decade [1]. To improve planning and evaluate the impact of integrating these inverter-based resources (IBRs) with the grid, there is a need to develop adequate solar and wind farm models that can be included in power system simulation and analysis software for representing the dynamic response and behavior of the farms. Solar and wind farms usually consist of several generation units all linked together through a collector network, with each unity connecting via an inverter and pad-mounted transformers. As the size and number of PV plants and wind farm increases, it becomes challenging for power system planners to study their impact on the power system, since it is not practical to represent all individual inverters, transformers and feeders to conduct simulations. In simplifying the process of equivalencing wind farms with Type 1 and Type 2 wind turbine generators (WTG), [3] argues that the machine impedance is extremely high compared to the collector cable impedance, thus, obviating the need to consider the collector in equivalencing wind power plants. In [4], a Thevenin equivalent of a wind farm with Type 3 WTGs is developed. In [5], a real-world solar farm is simulated to study the impact of the collector system on short circuit currents. The authors argued that the impact of the collector network on short circuit response is negligible by comparing the fault response of the solar farm with that of a lumped model of the solar farm.

This paper extends the work presented in [5] by studying the impact of aggregating the collector network on a solar farm and a wind farm. Two different aggregation techniques are studied. In the first, the collector network is represented as an equivalent impedance and a shunt capacitance. In the second, just as in [3], [5], it is assumed that the impact of the collector network impedance is negligible. The aggregated farm models from both techniques are compared to the detailed farm models for various faults and the results are presented. Additionally, a sensitivity analysis is performed to observe the impact of increasing collector feeder length on the models.

This material is based upon work supported by the U.S. Department of Energy's Office of Energy Efficiency and Renewable Energy (EERE) under Wind Energy Technologies Office (WETO) Agreement Number 39419.

II. Power System Models

To demonstrate the effect of an equivalent collector network on large farms, three different cases are studied using a solar farm and a wind farm.

- A solar farm in grid-following mode
- A wind farm in grid-following mode
- The same wind farm, but in grid-forming mode

All models used for the studies in this paper are developed in MATLAB Simulink.

A. Solar Farm

The solar farm modeled for this study is a real-world solar farm that consists of 34 IBRs connected in 5 strings as shown in Fig. 1. Each string consists of 6 or 7 solar PV units and

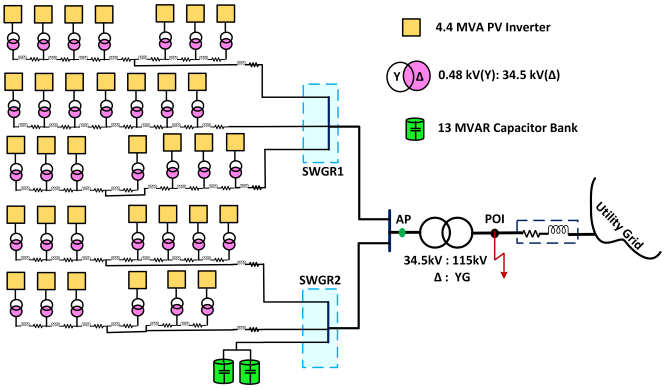

Fig. 1. One-line diagram of solar farm.

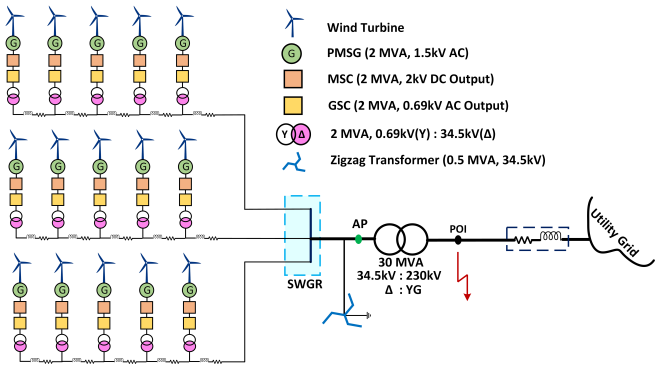

Fig. 2. One-line diagram of wind farm.

is each connected to the collector circuit through 4.4 MVA $480V/34.5kV$, Y/Δ pad-mounted transformer with 7.5% impedance. The average collector line length is 0.35 km. Each of the units is rated at 4.4 MVA. A 150 MVA $34.5/115kV$, Δ/Yg step up transformer with a 12% impedance connects the solar farm to the grid. The high-voltage bus of this transformer is defined as the point of interconnection (POI). Voltage and current measurements are recorded from the aggregating point (AP).

All 34 inverters are set to operate in grid-following mode providing the rated power at unity power factor. Reactive power support comes from a 26 MVar capacitor bank located at the collector circuit. The inverters are connected to the collector system through their LCL filter and interfacing transformer. The LCL filter parameters are calculated using the procedure outlined in [6] and the record of the inverter model and settings can be found in [5]. The average collector line length is 0.35 km, and the longest line is 0.85 km. The farthest unit is 2.8 km from the POI.

B. Wind Farm

Fig. 2 shows the one-line diagram of the wind farm used in case 2 and 3. The type-4 wind farm consists of 15 turbine units connected in 3 strings (i.e. 5 wind turbines in a string). Each wind turbine unit is connected to a 1.5 kV AC permanent magnet synchronous generator (PMSG). The generator speed is controlled through a machine-side converter (MSC), while the control of the DC bus voltage and reactive power is achieved via the grid-side converter (GSC). The PMSG and MSC used in this paper follow the detailed description provided in chapter 6 of [7]. The GSC is capable of operating in grid-forming or grid-following control mode. A detailed description of this GSC, filter parameters, and control diagram can be found in [8]. Each unit is rated at 2 MVA and is connected to the collector circuit through a 2 MVA $690V/34.5kV$, Y/Δ transformer. To create a path for ground faults in the collector network, a 0.5 MVA zigzag transformer is connected after the switch gear (SWGR). The farm establishes the average collector length based on measurement data obtained from similar farms using Google Earth. In this configuration, each wind turbine unit is positioned with a minimum spacing of 0.48 km, exceeding three times the rotor diameter of a typical 2 MW wind turbine. The average collector length is 0.69 km, and the farthest unit is 3.36 km away from the POI.

III. Aggregating the Collector System

In this section, the process of aggregating the wind and solar farms for short circuit analysis is described. Two different aggregation techniques are considered, leading to the formulation of two equivalent models: "Equivalent Model A" and "Equivalent Model B".

A. Equivalent Model A

In this model, the collector network of the farm is represented with a positive and zero sequence equivalent impedance, Z_{Col} and an equivalent shunt capacitance, B_{col}. In MATLAB, this is modeled as a three-phase transmission line with a single PI section. Z_{Col} and B_{col} are calculated using the equations derived in [9]–[11] by assuming that the voltage amplitudes at the collector system buses are the same and that the currents in the collector system susceptance are negligible. Table I shows the calculated impedance values for the solar and wind farms. In addition, all the inverters and transformers are lumped into a single inverter and transformer. For the Solar farm in Fig. 1, this will be all 34 inverters (4.4 MVA each) and transformers combined to give a single inverter and transformer as shown in Fig. 3. The transformer is scaled to a rating of 34×4.4 MVA. Similarly, for the Wind farm in Fig. 2, the "Equivalent Model A" is a single 30 MVA inverter connected through a single interfacing transformer as shown in Fig. 4. The LCL filters for the inverters are also scaled in a similar way using a change of base.

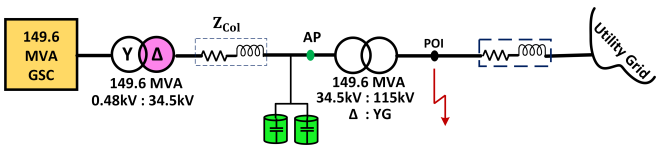

Fig. 3. Equivalent model A of the 34 unit solar farm.

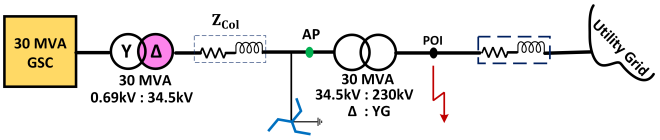

Fig. 4. Equivalent model A of the 15 unit wind farm.

TABLE I
POSITIVE AND ZERO SEQUENCE EQUIVALENT IMPEDANCE (%) USED FOR MODEL A

Parameter	Solar Farm	Wind Farm
$R_0(\Omega/Km)$	0.0625	0.1010
$R_1(\Omega/Km)$	0.0230	0.0226
$X_0(H/Km)$	6.4717e-4	7.7707e-4
$X_1(H/Km)$	6.2959e-4	2.3021e-4
$B_0(F/Km)$	3.0150e-4	8.2471e-7
$B_1(F/Km)$	3.0150e-4	1.3555e-7

B. Equivalent Model B

In this model, all the inverters and transformers are also lumped into a single inverter and transformer. However, the impedance of the collector network is neglected. This aggregation method is presented as a lumped model in [5] and assumes that the collector network on fault response is negligible.

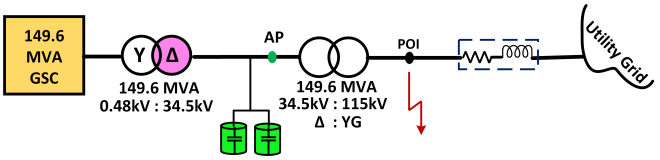

Fig. 5. Equivalent model B of the solar farm.

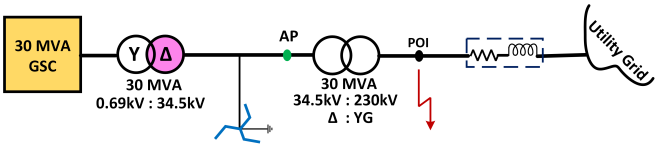

Fig. 6. Equivalent model B of the wind farm.

IV. RESULT

To observe the impact of the collector network in an IBR farm, this paper compares the fault current output of the three models (the detailed model, equivalent model A, and equivalent model B). At the POI, three phase (3ph), line to line (LL), and single line to ground (SLG) faults are applied. The output voltage is measured at point AP. To compare each equivalent model with the detailed model, the root mean square error (RMSE) was calculated using eqn (1)

$$RMSE = \sqrt{\frac{\sum_i^N \left(\frac{S1_i - S2_i}{S2_i}\right)^2}{N}} \quad (1)$$

where $S1$ is the output from the detailed model, $S2$ is the output from the aggregated model, i is the sample index , and N is the total number of samples.

A. Case 1: Solar farm in Grid-following mode

With the solar farm connected in grid-following mode, a fault is applied at time $t = 2.0s$ for a duration of $0.2s$. Fig. 7 shows the plot of the measured voltage of the detailed model and the aggregated models during a LL fault. The top plot compares the voltages of the detailed model and the "equivalent model A", while the bottom plot compares the voltages of the detailed model and the "equivalent model B". The corresponding current plot during the LL fault is shown in Fig. 8. For the duration of the fault, the RMSE values when comparing the detailed model with "Equivalent model A" is 0.08% for the voltage magnitude and 0.02% for the current magnitude. The RMSE values when comparing the detailed model with the "equivalent model B" is 0.24% for the voltage magnitude and 0.33% for the current magnitude. Table II shows the RMSE values for all the fault types simulated in this case. For the model with the equivalent collector impedance, the RMSE values calculated are all less than 0.5%. For the aggregated model any representation of the collector network, the RMSE values are between 0.1% and 0.33%.

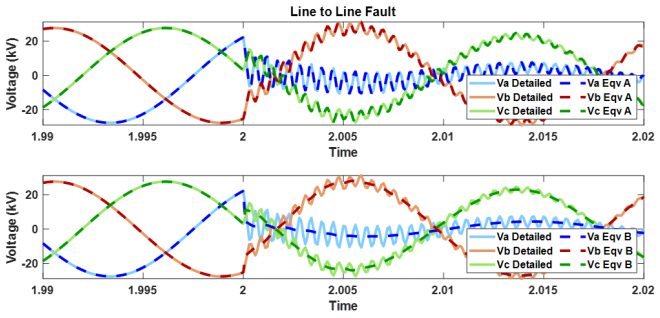

Fig. 7. Voltage of the solar farm during a line to line fault for the detailed model, a)equivalent model A, and b)equivalent model B.

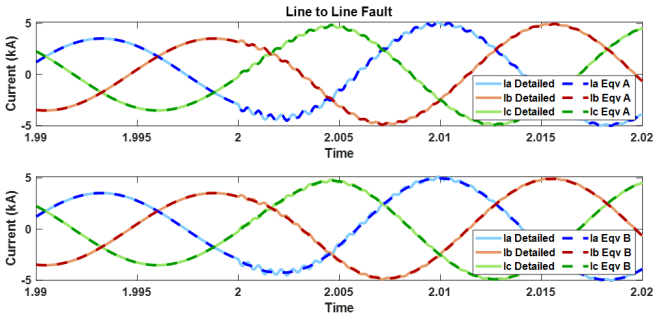

Fig. 8. Current of the solar farm during a line to line fault for the detailed model, a)equivalent model A, and b)equivalent model B.

B. Case 2: Wind farm in Grid-following mode

With the wind farm connected in grid-following mode, a fault is applied at time $t = 2.0s$ for a duration of $0.2s$. Fig. 9 and Fig. 10 shows the plot of the measured voltage and current output of the detailed model and the aggregated models for a 3ph fault. The top plot compares the three-phase voltage of

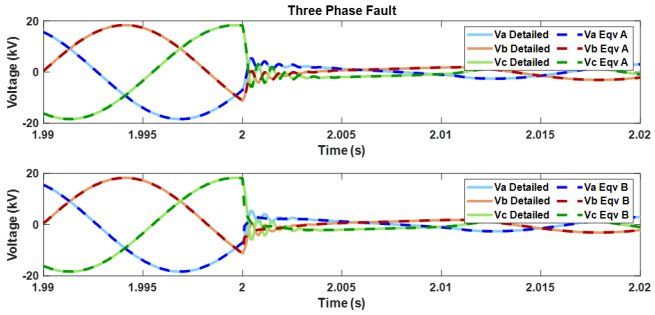

Fig. 9. Voltage of the wind farm during a 3-phase fault (grid following mode).

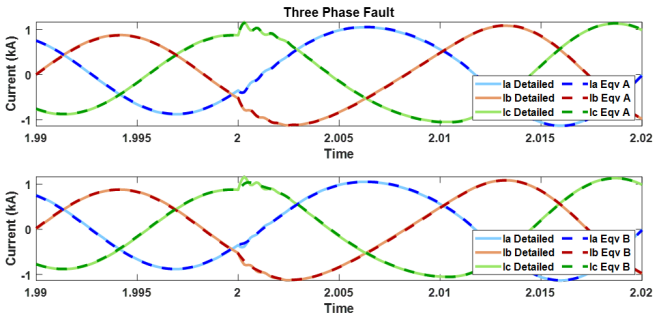

Fig. 10. Current of the wind farm during a 3ph fault (grid following mode).

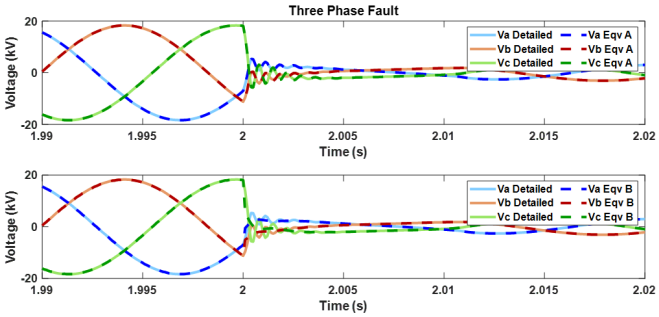

Fig. 11. Voltage of the wind farm during a 3-phase fault (grid forming mode).

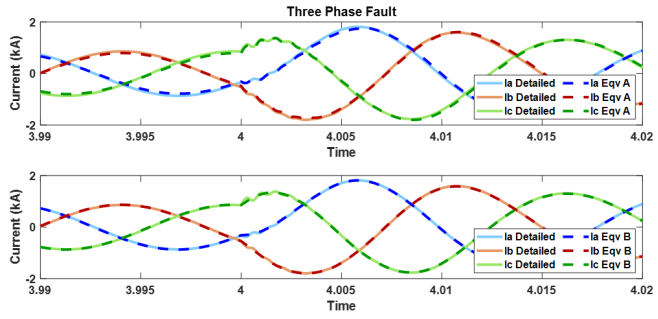

Fig. 12. Current of the wind farm during a 3-phase fault (grid forming mode).

the detailed model and the "equivalent model A", while the bottom plot compares the three-phase current of the detailed model to that of the "equivalent model B". The voltage and current magnitude RMSE values of the "equivalent model A" are 0.46% and 0.31% respectively, and the voltage and current magnitude RMSE values for the "equivalent model B" are 0.32% and 0.31% respectively. The RMSE values for all the fault types simulated in this case are also shown in Table II. Just as in the solar farm in case 1, the RSME values are quite low. This suggests that for a farm operating in grid following mode, with a collector network size similar to the wind farm in Fig. 2, any of the aggregated models will be accurate enough for short circuit studies.

C. Case 3: Wind farm in Grid-forming mode

With the wind farm connected in grid-forming mode, the faults are applied at time $t = 4.0s$ for a duration of 0.2. Fig. 11 and Fig. 12 show the measured output voltage and current for the detailed model and the aggregated models for a 3ph fault. The top plot compares the three-phase voltage of the detailed model and the "equivalent model A", while the bottom plot compares the three-phase current of the detailed model to that of the "equivalent model B". The voltage and current magnitude RMSE values of the "equivalent model A" are 0.80% and 1.97% respectively, and the voltage and current magnitude RMSE values for the "equivalent model B" are 0.47% and 0.36% respectively. Table II shows the RMSE values for all the fault types simulated in this case. For the aggregated model with the equivalent collector impedance, the RMSE values are more than the aggregated model without the collector network. For both models, the RMSE values calculated for are all less than 4%.

TABLE II
RMSE FOR THE SOLAR FARM IN GRID FOLLOWING MODE (%)

Model	Case 1		Case 2		Case 3	
Model	Eqv A	Eqv B	Eqv A	Eqv B	Eqv A	Eqv B
$3\ ph\ \|V\|$	0.10	0.29	0.46	0.32	0.80	0.47
$3\ ph\ \|I\|$	0.01	0.10	0.31	0.31	1.97	0.36
$LL\ \|V\|$	0.08	0.24	0.42	0.27	1.04	0.35
$LL\ \|I\|$	0.02	0.33	0.31	1.42	2.60	1.55
$SLG\ \|V\|$	0.01	0.22	0.25	0.15	0.56	0.22
$SLG\ \|I\|$	0.02	0.21	0.50	0.84	3.42	0.36

V. Impact of Collector Feeder Length

As the scale of interconnected IBR farms grow in our grid today, the units become spaced further apart. Consequently, there is an increase in the length and impedance associated with the collector network. To study the impact of the collector network length on each type of aggregation, the length of the collector feeders of the solar and wind farms were increased by multiplying the original feeder lengths by factor l.

In the detailed model of the solar farm operating in grid-following mode, the average collector line length is 0.35 km, for a factor $l = 10$, the average line length is increased to 3.5 km. With 3ph, LL, SLG faults simulated in all three cases for a factor l ranging from 2 to 10, the maximum voltage and current RMSEs are calculated, and the values are plotted and shown in Fig. 13. Although the voltage and current RMSE for

both aggregated models increases with the increased collector line length, the rate of increase for 'Eqv A' is less than that of 'Eqv B'. When the collector length is 10 times the original length, the current error for 'Eqv B' is above 8% while the current error for 'Eqv A' is below 3%. This suggests that for solar farms with long collector line lengths, the 'equivalent model A' aggregation model will be a more accurate model for short circuit studies than that of 'equivalent model B'. A similar pattern is observed in the case of the wind farm operating in grid following mode. For the wind farm, average collector length is 0.69 km, and for a factor of $l = 9$, the average line length is increased to 6.21 km. Fig. 14 shows the maximum voltage and current RMSE at different line lengths when the wind farm operates in grid following mode. When the collector line length is 9 times the original length, the current error for 'Eqv B' is above 10%, however, for 'Eqv A' the error is below 1%. When the wind farm is in grid forming mode, the maximum voltage and current RMSE increases as the line length increases for the 'Eqv B' model. However, for the 'Eqv A' model, the voltage error is within 0.8% and 3% while the current error is within 3% and 7% error for all line lengths simulated. Fig. 15 shows the maximum voltage and current RMSE at different line lengths when the wind farm operates in grid forming mode.

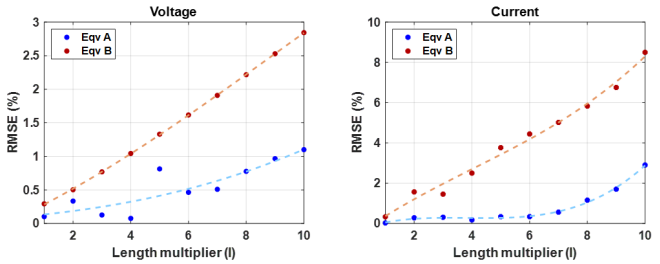

Fig. 13. Maximum voltage and current error of the solar farm with increasing line lengths.

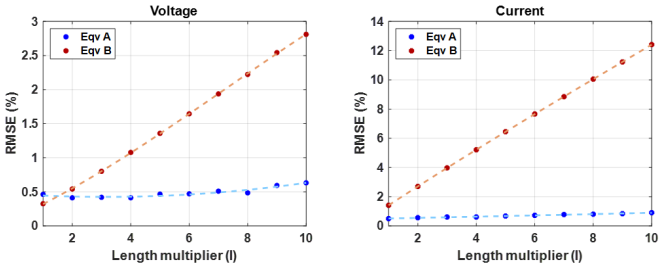

Fig. 14. Maximum voltage and current error of the wind farm with increasing line lengths (grid following mode).

VI. Conclusions

In this paper, a solar farm and a wind farm are simulated in MATLAB (Simulink) to study the impact of collector network aggregation on short circuit currents. Two different aggregation techniques are discussed. One assumes that the impact of the collector network impedance is negligible while the other

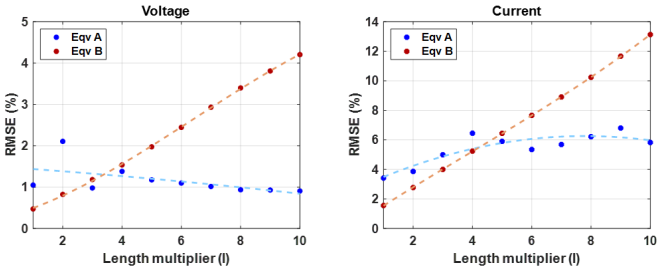

Fig. 15. Maximum voltage and current error of the wind farm with increasing line lengths (grid forming mode).

represents the collector network as an equivalent impedance and a shunt capacitance. Several faults are simulated on the solar farm and wind farm as well as on both of the aggregated models for each farm. The difference between the output voltages and currents of the farms and their aggregated versions are compared. The results show that when the solar and wind farms are operating in grid following mode, the aggregated model with an equivalent impedance representing the collector network is more accurate for short circuit studies than the aggregated model that ignores the effects of the collector network.

References

[1] Center for Sustainable Systems University of Michigan, "U.S. renewable energy factsheets," *Center for Sustainable Systems, University of Michigan*, 2023.

[2] S. T. Ojetola, R. Darbali-Zamora, and F. Wilches-Bernal, "An advanced voltage regulation control for distributed wind turbine generators," in *2023 IEEE Power and Energy Society Innovative Smart Grid Technologies Conference (ISGT)*, 2023, pp. 1–5.

[3] S. M. Brahma, M. Chaudhary, and S. J. Ranade, "Some findings about equivalencing windfarms with type 1 and type 2 induction generators," in *2011 North American Power Symposium*, 2011, pp. 1–6.

[4] J. Brochu, C. Larose, and R. Gagnon, "Validation of single- and multiple-machine equivalents for modeling wind power plants," *IEEE Transactions on Energy Conversion*, vol. 26, no. 2, pp. 532–541, 2011.

[5] T. Patel, S. Brahma, and M. J. Reno, "Aggregation of solar and type 4 wind farms for short circuit studies," in *2023 IEEE Power and Energy Society Innovative Smart Grid Technologies Conference (ISGT)*, 2023, pp. 1–5.

[6] M. Dursun and M. K. Dosoglu, "LCL filter design for grid connected three-phase inverter," in *2018 2nd International Symposium on Multidisciplinary Studies and Innovative Technologies (ISMSIT)*, 2018, pp. 1–4.

[7] M. Singh and S. Santoso, "Dynamic models for wind turbines and wind power plants," 10 2011. [Online]. Available: https://www.osti.gov/biblio/1028524

[8] S. M. Hossain, T. Patel, S. Brahma, and M. J. Reno, "Modeling of hybrid farm in grid following and grid forming modes for short circuit studies," in *2024 IEEE Green Technologies Conference (GreenTech)*, 2024, pp. 1–5.

[9] E. Muljadi, C. P. Butterfield, A. Ellis, J. Mechenbier, J. Hochheimer, R. Young, N. Miller, R. Delmerico, R. Zavadil, and J. C. Smith, "Equivalencing the collector system of a large wind power plant," in *2006 IEEE Power Engineering Society General Meeting*, 2006, p. 9 pp.

[10] E. Muljadi, S. Pasupulati, A. Ellis, and D. Kosterov, "Method of equivalencing for a large wind power plant with multiple turbine representation," in *2008 IEEE Power and Energy Society General Meeting - Conversion and Delivery of Electrical Energy in the 21st Century*, 2008, pp. 1–9.

[11] Y. Yang and X. Zha, "Aggregating wind farm with DFIG in power system online analysis," in *2009 IEEE 6th International Power Electronics and Motion Control Conference*, 2009, pp. 2233–2237.